Importance of MM Polarization in QM/MM Studies of Enzymatic Reactions: Assessment of the QM/MM Drude Oscillator Model

*Abir Ganguly, Eliot Boulanger and Walter Thiel**

Max-Planck-Institut für Kohlenforschung, Kaiser-Wilhelm-Platz 1, 45470 Mülheim an der Ruhr, Germany

Supporting information

Table S1. Reaction energies (ΔE) and activation energies ($\Delta E^{\ddagger}$) of the CM-catalyzed reaction for five snapshots with different initial configurations calculated using the QM/MM-DO and QM/MM-ADD models. The QM region is modeled with the semiempirical OM2 Hamiltonian. All values in kcal/mol.

	QM/MM-DO		QM/MM-ADD			
snapshot	ΔE	$\Delta E^{\ddagger}$	ΔE	$\Delta E^{\ddagger}$	ΔΔE	$\Delta\Delta E^{\ddagger}$
1	-27.3	13.5	-28.9	12.7	1.6	0.8
2	-24.1	13.4	-24.9	13.7	0.8	-0.3
3	-25.2	17.6	-24.6	16.4	-0.6	1.2
4	-27.8	15.5	-25.6	14.8	-2.2	0.7
5	-27.0	13.3	-26.8	12.8	-0.2	0.5
Mean	-26.3	14.7	-26.2	14.1	-0.1	0.6

Table S2. RMSDs between optimized reactant (R), transition state (TS), and product (P) geometries of the CM-catalyzed reaction obtained using the QM/MM-DO and QM/MM-ADD models. The geometries are derived from calculations in which the QM region is described at the B3LYP/def2-SVP level. RMSD values in Å.

snapshot	R	TS	P
1	0.05	0.05	0.06
2	0.05	0.04	0.08
3	0.05	0.07	0.13
4	0.04	0.06	0.09
5	0.03	0.04	0.07
Mean	0.05	0.05	0.09

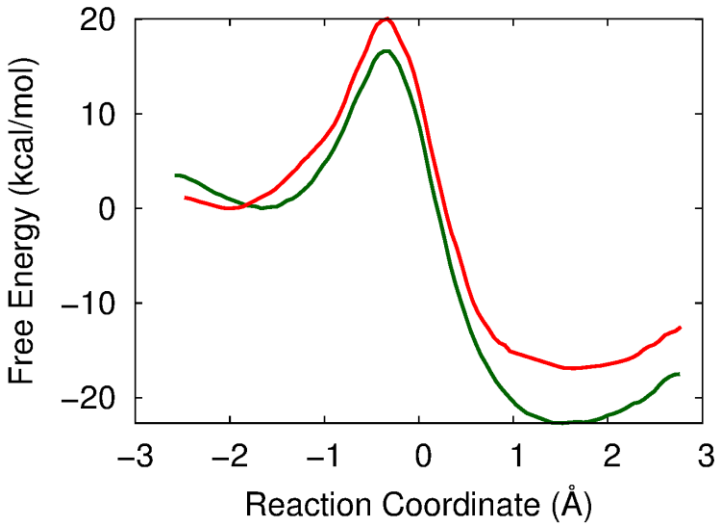

Figure S1. Free energy profiles for the CM-catalyzed reaction obtained using QM/MM-DO (red) and QM/MM-ADD (green) models. The QM region is modeled with the semiempirical OM2 Hamiltonian.

Table S3. Reaction energies (ΔE) and activation energies ($\Delta E^{\ddagger}$) of the PHBH-catalyzed reaction for five snapshots with different initial configurations calculated using the QM/MM-DO and QM/MM-ADD models. The QM region is modeled with the semiempirical OM2 Hamiltonian. All values in kcal/mol.

	QM/MM-DO		QM/MM-ADD			
snapshot	ΔE	$\Delta E^{\ddagger}$	ΔE	$\Delta E^{\ddagger}$	$\Delta\Delta E$	$\Delta\Delta E^{\ddagger}$
1	-54.0	7.1	-56.0	8.7	2.0	-1.6
2	-56.0	7.0	-57.9	6.1	1.9	0.9
3	-53.0	4.8	-59.4	3.8	6.4	1.0
4	-64.2	6.6	-66.0	6.2	1.8	0.4
Mean	-56.8	6.4	-59.8	6.2	3.0	0.2

Table S4. RMSDs between optimized reactant (R), transition state (TS), and product (P) geometries of the PHBH-catalyzed reaction obtained using the QM/MM-DO and QM/MM-ADD models. The geometries are derived from calculations in which the QM region is described at the B3LYP/def2-SVP level. RMSD values in Å.

snapshot	R	TS	P
1	0.47	0.49	0.52
2	0.39	0.21	0.22
3	0.43	0.19	0.22
4	0.22	0.19	0.19
Mean	0.38	0.27	0.29

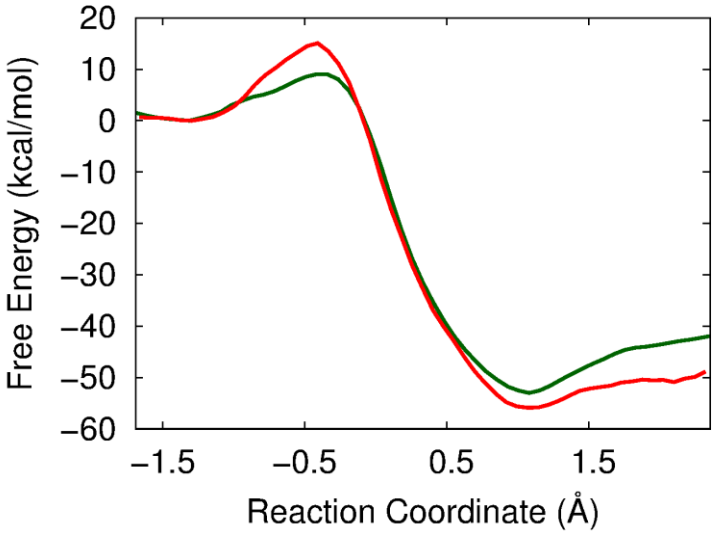

Figure S2. Free energy profiles for the PHBH catalytic reaction obtained using QM/MM-DO (red) and QM/MM-ADD (green) models. The QM region is modeled with the semiempirical OM2 Hamiltonian.

Computational details: QM/MM string simulations and umbrella sampling simulations

Chorismate Mutase

The strings were constructed in the space of two reaction coordinates, the C9-O8 distance and C1-C13 distance of CHO (Scheme 1). 30 equally spaced images were considered along the string. The initial string was constructed from QM/MM-ADD optimized geometries along the reaction path of snapshot 1. In the simulations where the QM region was treated at the DFT level, MD trajectories were run at each image and each iteration, the length of which varied from 0.1ps (initially) to 1 ps (during the final few iterations), and the string was considered converged after 26 iterations. In analogous simulations where the QM region was treated at the semiempirical OM2 level, MD trajectories were run at each image and each iteration, the length of which varied from 0.2 ps (initially) to 5 ps (during final few iterations), and the string was considered converged after 33 iterations. Force constants ranging from 100 to 300 kcal/(mol $Å^2$) were used for the restraining potentials. The string simulations were performed using only the QM/MM-ADD model.

One-dimensional US simulations were performed on representative structures taken along the MFEP obtained from the string simulations, using the QM/MM-DO and QM/MM-ADD models. In the US simulations, 30 windows were considered and at each window MD trajectories were propagated for 1 ps and 5 ps in the simulations at the DFT and semiempirical OM2 levels, respectively.

p-Hydroxybenzoate hydrolase

The strings were constructed in the space of two reaction coordinates, the O_d-O_p distance and O_d-C_m distance in the PHBH active site (Scheme 2). 30 equally spaced images were considered along the string. The initial string was constructed from QM/MM-ADD optimized geometries along the reaction path of snapshot 1. In the simulations where the QM region was treated at the DFT level, MD trajectories were run at each image and each iteration, the length of which varied from 0.1ps (initially) to 1 ps (during the final few iterations), and the string was considered converged after 31 iterations. In analogous simulations where the QM region was treated at the semiempirical OM2 level, MD trajectories were run at each image and each iteration, the length of which varied from 0.2 ps (initially) to 5 ps (during final few iterations), and the string was considered converged after 37 iterations. Force constants ranging from 100 to 300 kcal/(mol $Å^2$) were used for the restraining potentials. The string simulations were performed using only the QM/MM-ADD model.

One-dimensional US simulations were performed on representative structures taken along the MFEP obtained from the string simulations, using the QM/MM-DO and QM/MM-ADD models. In the US simulations, 57 windows were considered and at each window MD trajectories were propagated for 1 ps and 5 ps in the simulations at the DFT and semiempirical OM2 levels, respectively.

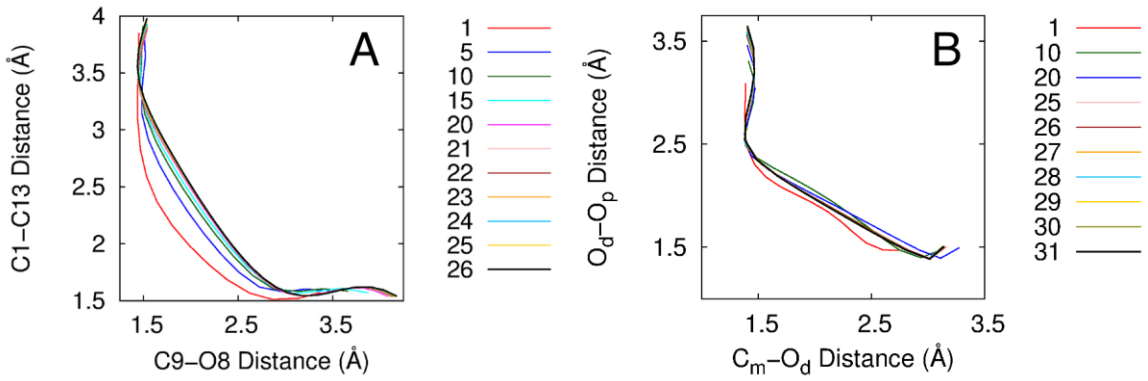

Figure S3. Convergence of the string simulations for the CM (A) and PHBH (B) catalyzed reactions. Strings from specific iterations are plotted in the space of the C9-O8 and C1-C13 reaction coordinates in case of CM, and of the C_m-O_d and O_d-O_p reaction coordinates in case of PHBH. The iterations are indicated in the explanation of the color code. Evidently, for both CM and PHBH, the respective strings exhibit negligible displacements during the final iterations, indicating their convergence. The simulations were performed at the QM(B3LYP/def2-SVP)/MM-ADD level.

Comment:

The string simulations at the QM/MM-ADD level can directly provide free energy data using WHAM analysis. In the case of CM, this procedure yields an activation free energy of $\Delta G^{\ddagger}$ = 15.4 kcal/mol and a reaction free energy of ΔG = -16.0 kcal/mol. These values are very similar to those obtained from the subsequent umbrella sampling simulations (ΔG = -15.1 kcal/mol; $\Delta G^{\ddagger}$ = 14.1 kcal/mol) described in the main paper.

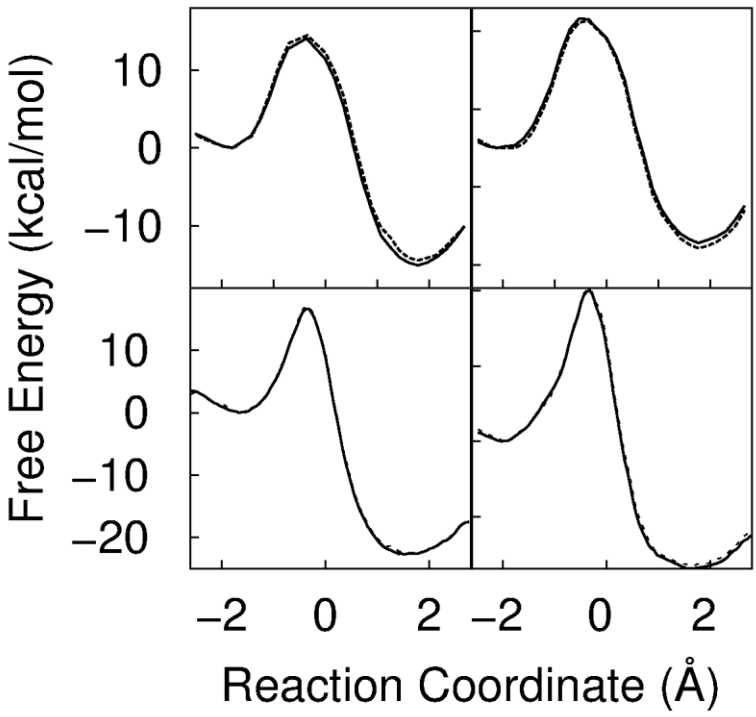

Figure S4. Convergence of the free energy profiles for the CM-catalyzed reaction calculated using the QM/MM-DO (A, C) and QM/MM-ADD (B, D) models. In (A) and (B), the profiles are obtained from DFT/MM calculations while in (C) and (D), the profiles are obtained from OM2/MM calculations. In (A-D), the solid and dashed lines correspond to free energy profiles calculated using 100% and 50% of the total data, respectively.

Energy decomposition analysis: Procedure

In an attempt to further disentangle the effects of MM polarization on the computed energies, we performed an energy decomposition analysis for each stationary point obtained at the QM/MM-DO level for chorismate mutase (CM). We adopted the following procedure.

Step 1. Remove the QM region and perform a DO calculation to determine initial coordinates of the Drude particles. Calculate the MM-DO energy of this system. $[E_{DO_0}^{MM}]$

Step 2. Insert the QM region and calculate the QM energy in the field of the MM-DO region, with the Drude particles in their precomputed positions. $[E_{DO_0}^{QM}]$

Step3. Optimize the positions of the Drude particles in the presence of the QM region and calculate the QM energy in the field of the optimized MM-DO region and also compute the corresponding MM-DO energy. $[E_{DO_1}^{QM}]$ and $[E_{DO_1}^{MM}]$.

Step 4. Calculate the QM energy at the QM/MM level without Drude particles. $[E_{MM}^{QM}]$

$\Delta QM_1 = E_{DO_0}^{QM} - E_{MM}^{QM}$ measures the change in the QM energy due to the presence of the unrelaxed Drude particles; $\Delta QM_2 = E_{DO_1}^{QM} - E_{DO_0}^{QM}$ measures the change in the QM energy due to the optimization of the Drude particles; $\Delta QM_3 = E_{DO_1}^{QM} - E_{MM}^{QM}$ measures the total effect of MM polarization on the QM energy; $\Delta MM = E_{DO_1}^{MM} - E_{DO_0}^{MM}$ measures the change in the MM-DO energy caused by the presence of the QM region.

This energy decomposition analysis was performed for all five snapshots of CM. The results are summarized below. The energy differences are reported as such (Table S5) and relative to the corresponding values of the reactant state (Table S6).

Table S5. Energy decomposition analysis for chorismate mutase. Energy differences (kcal/mol) for the reactant (R), transition state (TS), and product (P) of the five snapshots considered.

snap	state	ΔQM_1	ΔQM_2	ΔQM_3	ΔMM
1	R	168.20	-194.13	-25.93	89.09
	TS	170.87	-197.68	-26.82	90.74
	P	166.55	-190.36	-23.81	86.87
2	R	166.07	-193.44	-27.37	83.54
	TS	169.60	-195.73	-26.13	84.85
	P	164.98	-188.83	-23.85	81.28
3	R	155.50	-190.81	-35.31	89.18
	TS	158.47	-194.14	-35.66	90.78
	P	154.50	-187.42	-32.92	87.15
4	R	171.25	-198.93	-27.68	86.68
	TS	173.07	-201.75	-28.68	88.34
	P	168.26	-193.40	-25.14	83.98
5	R	179.95	-196.92	-16.97	82.35
	TS	181.92	-199.66	-17.74	83.66
	P	177.94	-192.01	-14.07	79.83

Comments:

In a system of the size of chorismate mutase, MM polarization has large effects on the QM energy of the stationary points. Upon inclusion of unrelaxed Drude particles, the QM energy increases by typically 160-170 kcal/mol. Optimization of the position of the Drude particles at the QM/MM level lowers the QM energy by typically 190-200 kcal/mol. Overall, accounting for MM polarization lowers the QM energy by about 20-30 kcal/mol.

Considering the individual energy differences for the stationary points in each snapshot, the values for reactant, transition state, and product show only minor variations (mostly less than 5 kcal/mol). Hence, the effects of MM polarization on the computed energies are large in absolute terms, but they do not change much during the reaction. This is quantified in Table S6 by presenting the changes relative to the reactant.

Inspection of Table S6 shows that the inclusion of unrelaxed Drude particle raises the relative QM energy of the transition state by 1.8-3.5 kcal/mol while lowering that of the product by 1.0-3.0 kcal/mol. Optimization of the position of the Drude particles at the QM/MM level causes shifts in the opposite direction: the relative QM energy of the transition state decreases by 2.3-3.6 kcal/mol while that of the product increases by 3.4-5.5 kcal/mol. As a consequence, the overall effect of MM polarization of the relative QM energies is rather small, ranging from -1.0 to +1.2 kcal/mol for the transition state and from 2.1 to 3.5 kcal/mol for the product.

Table S6. Energy decomposition analysis for chorismate mutase. Energy differences (kcal/mol) relative to the reactant, for the transition state and the product of the five snapshots considered.

	Transition state				Product			
	ΔQM_1	ΔQM_2	ΔQM_3	ΔMM	ΔQM_1	ΔQM_2	ΔQM_3	ΔMM
1	2.7	-3.6	-0.9	1.7	-1.7	3.8	2.1	-2.2
2	3.5	-2.3	1.2	1.3	-1.1	4.6	3.5	-2.3
3	3.0	-3.3	-0.4	1.6	-1.0	3.4	2.4	-2.0
4	1.8	-2.8	-1.0	1.7	-3.0	5.5	2.6	-2.7
5	2.0	-2.7	-0.8	1.3	-2.0	4.9	2.9	-2.5

Computational details: Scans of energy profiles

For CM, the scans of the energy profiles were performed along the coordinate $\xi = d(C9 - O8) - d(C1 - C13)$; ξ spanned the range from -2.4 Å (reactant) to 2.4 Å (product). The scans were initiated from the fully optimized reactant state, and ξ was increased in steps of 0.25 Å until the product state was reached. For each point along the scan, the difference between the two distances (C9-O8) and (C1-C13) was held fixed to the corresponding value of ξ and the geometry was fully optimized (optimization criteria: Cartesian gradient=0.00045 au; Cartesian displacement=0.0018 au). Once the product state was reached, the product geometry was fully optimized (without any geometry constraints) and the PES scan was conducted in the backward direction to reach the reactant state. This approach of performing PES scans in forward and backward direction was repeated until the energy profiles obtained from either direction were identical. For PHBH, the PES scans were performed in the same fashion along the reaction coordinate $\xi = d(O_d - O_p) - d(C_m - O_d)$, spanning the range from -1.7 Å (reactant) to 1.3 Å (product).